



## SWIFT-XRT-CALDB-09

Release Date: June 7<sup>th</sup>, 2011

Prepared by: Andrew Beardmore<sup>1</sup>, Claudio Pagani<sup>1</sup>, Sergio Campana<sup>2</sup>

Date revised: May 17<sup>th</sup>, 2011

Revision: 15

Revised by: Andrew Beardmore

<sup>1</sup> Leicester, <sup>2</sup> INAF-OAB

# SWIFT XRT CALDB RELEASE NOTE

## SWIFT-XRT-CALDB-09:

### Response matrices and Ancillary Response Files

Table 1: Files to be released:

Filename	Mode	Grade	Substrate* voltage (V)	Release Date
swxwt0to2s6_20010101v013.rmf	WT	0-2	6	07-Jun-2011
swxwt0to2s6_20010101v013.arf	WT	0-2	6	07-Jun-2011
swxwt0s6_20010101v013.rmf	WT	0	6	07-Jun-2011
swxwt0s6_20010101v013.arf	WT	0	6	07-Jun-2011
swxpc0to12s6_20010101v012.rmf	PC	0-12	6	07-Jun-2011
swxpc0to12s6_20010101v012.arf	PC	0-12	6	07-Jun-2011
swxpc0s6_20010101v012.rmf	PC	0	6	07-Jun-2011
swxpc0s6_20010101v012.arf	PC	0	6	07-Jun-2011

\*The substrate voltage was permanently raised from  $V_{ss} = 0$  V to  $V_{ss} = 6$  V on 2007 August 30 (see below).

# Scope of Document

This note describes the release of updated *Swift*-XRT Windowed Timing (WT) and Photon Counting (PC) mode redistribution matrix files (RMFs) and ancillary response files (ARFs), appropriate for data taken after the CCD substrate voltage change on 2007-Aug-31 (see Table 1).

## Introduction

The XRT effective area is made up of three main components: the mirror effective area, the filter transmission and the CCD quantum efficiency (QE). The QE is included directly in the redistribution matrix files (RMFs) while the ancillary response files (ARFs) contain the mirror effective area and the filter transmission.

Observation-specific ARF files are produced by the `XRTMKARF` task (part of the `XRTDAS-HEADAS` software). This task corrects the nominal (on-axis, infinite extraction region) ARF file from the CALDB for the effects of telescope vignetting and, optionally (`psfflag=yes`), for PSF losses incurred when finite sized extraction regions are used in point source analysis. Additional corrections for CCD defects (caused by ‘bad columns’ or ‘hot-pixels’) can be made with the inclusion of an exposure map (with the option `expofile=filename.img`), which can automatically be generated by the data analysis pipeline. The task can also generate ARFs for extended sources (option `extended=yes`), such as clusters of galaxies or supernova remnants.

As well as accounting for the CCD QE, the RMFs model the response of the detector to incident X-rays and are mode, grade and epoch dependent (see below).

## Motivation behind this release

The release makes available two new improvements to the XRT performance: 1) the PC mode QE is more accurately described for data taken after 2007-Aug-31; 2) the XRT spectral resolution is improved significantly.

The XRT suffered a thermoelectric cooler power supply failure shortly after launch which meant the CCD could not be operated at the expected nominal temperature of  $-100^{\circ}\text{C}$ . However, by carefully controlling the spacecraft pointing during pre-planned science observations the CCD can be passively cooled to acceptable temperatures in the range  $\sim -75$  to  $-50^{\circ}\text{C}$  (Kennea et al. 2005, SPIE, 5898, 329).

Furthermore, laboratory testing showed that by raising the CCD substrate voltage from  $V_{ss} = 0\text{ V}$  to  $V_{ss} = 6\text{ V}$  the thermally induced dark current in the CCD could be reduced, allowing the CCD to operate a few degrees warmer before excessive hot pixels compromise data (Godet et al., 2009, A&A, 494, 775). Because of this, the XRT CCD substrate voltage was permanently raised to  $V_{ss} = 6\text{ V}$  on 2007 August 30 (at 14:28UT).

However, raising the substrate voltage caused the CCD depletion depth to decrease slightly which, in turn, altered the QE at high energies and just below the Si edge ( $\sim 1.5 - 1.84\text{ keV}$ ). The changes in QE were addressed for WT mode in the previous RMF/ARF CALDB release (see release note `SWIFT-XRT-CALDB-09.v14`) and are addressed for PC mode in this release.

Over time, the accumulated radiation dose and high-energy proton interactions cause damage to the CCD (in the imaging area, the store frame area and the serial register) resulting in a build-up of charge traps (i.e. faults in the Si crystalline structure of the CCD which hold onto some of the charge released during an X-ray interaction). The deepest traps are responsible for the strongest line FWHM degradation, with the line shape then showing a more pronounced low energy wing. The most serious of these charge traps can cause a loss of up to  $\sim 600\text{ eV}$  at  $6\text{ keV}$  and  $\sim 300\text{ eV}$  at  $1.856\text{ keV}$  from the incident X-ray energy, although typical values are very much smaller.

While we released a set of broadened WT and PC RMFs to account for the average line broadening behaviour up to 2008 (see the release notes `SWIFT-XRT-CALDB-09.v12` and `SWIFT-XRT-CALDB-09.v13`), our long term goal, realised with this release, was to improve the spectral resolution of the XRT by calibrating individual traps.

We have mapped the location and depths of the deepest traps on the CCD and updated the *Swift*-XRT `XRTCALCPI` software task to provide a trap specific energy scale reconstruction (see the gain file release note `SWIFT-XRT-CALDB-04.v10` for details and caveats). This has helped restore the spectral resolution (FWHM) of the detector from 175

eV in PC (225 eV in WT) at 1.86 keV in early 2010 to approximately 130 eV (for both modes).

**In this release, updated WT and PC RMFs and ARFs are made available appropriate for  $V_{ss} = 6$  V observations — i.e. those taken since 2007-Aug-31 — which have had the trap corrections applied.**

## RMF/ARF file naming scheme

The change in substrate voltage made it necessary to release two sets of RMF/ARF files, distinguished by the characters 's0' and 's6' in their filenames. The filenames also encode the XRT readout mode (WT or PC), the grade selection (0 – 2 or 0 for WT; 0 – 12 or 0 for PC) and the epoch the files are valid for use from. (Note, whilst all scientifically interesting  $V_{ss} = 6$  V data were taken after the permanent switch to  $V_{ss} = 6$  V operation, on 2007-Aug-31, the filename epoch predates this to account for the small amount of  $V_{ss} = 6$  V calibration data taken before this date.) The files released this time are, for WT mode:

<b>grade 0 – 2</b>	<b>grade 0</b>
<b>swxwt0to2s6_20010101v013.rmfmf</b>	<b>swxwt0s6_20010101v013.rmfmf</b>
<b>swxwt0to2s6_20010101v013.arfmf</b>	<b>swxwt0s6_20010101v013.arfmf</b>

and for PC mode :

<b>grade 0 – 12</b>	<b>grade 0</b>
<b>swxpc0to12s6_20010101v012.rmfmf</b>	<b>swxpc0s6_20010101v012.rmfmf</b>
<b>swxpc0to12s6_20010101v012.arfmf</b>	<b>swxpc0s6_20010101v012.arfmf</b>

## RMF generation

The Response Matrix Files (RMFs) are created by a Monte-Carlo simulation code (Godet et al. 2009, A&A, 494, 775, and references therein). This code models: transmission of the incident X-rays through the CCD electrode structure; photo-absorption in the active layers of the device (i.e. the depletion and field-free regions); charge cloud generation, transportation and spreading; silicon fluorescence and its associated escape peak; surface loss effects; mapping of the resultant charge-cloud to the detector pixel array; charge transfer efficiency; addition of electronic read-out noise; event thresholding and classification according to the specific mode of operation.

## Improvements specific to this release

### Photon Counting mode

For this release, PC mode RMFs have been created with an energy resolution which matches that provided by trap corrected data processing. Also, the CCD depletion depth (DD) has been modified to be more representative for  $V_{ss} = 6$  V operation. These goals were achieved as follows :

- The value of the readnoise used by the RMF simulation code was updated to  $7.5 e^-$ , which is more appropriate for the average XRT CCD operating temperature of  $-60^\circ\text{C}$ .
- The parallel and serial CTI coefficients were updated to  $8 \times 10^{-5}$  and  $5 \times 10^{-5}$ , respectively, at 5.895 keV, as measured from trap-free columns from the  $^{55}\text{Fe}$  corner source calibration data.
- The CTI coefficients were modified to introduce an energy dependence of the form  $CTI(E) \propto E^{-\alpha}$ , with  $\alpha = 0.2$ , calibrated on SNR 1E0102.2–7219 and Tycho SNR observations. The resultant FWHM of the new RMF is 125 eV at 1.86 keV and 200 eV at 5.895 keV, in agreement with 2008-Oct trap corrected data.
- The higher energy QE was lowered by changing the depletion depth to 20 microns. This value was determined by fitting RMFs of different depletion depths to the IACHEC cross-calibration source SNR G21.5–0.9 (see below).

- Further QE adjustments were made to ensure consistency with cross-calibration observations of the soft NS RX J1856.5–3754 at low energies, and a combination of 3C 273 and SNR G21.5–0.9 around the Si instrumental edge (see figure 1).
- The redistribution shelf level was modified to ensure consistency with the heavily absorbed sources SNR G21.5–0.9 and GRS 1741–2853, as well as the on-board  $^{55}\text{Fe}$  corner source data.

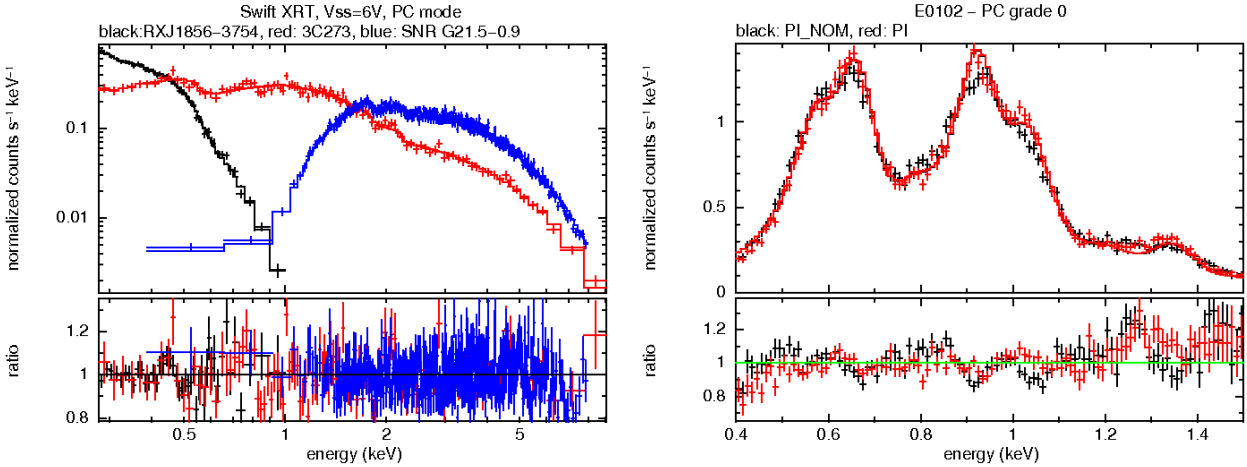


Figure 1: Left: Trap corrected, PC mode spectra from RX J1856.5–3754 (black), 3C 273 (red) and SNR G21.5–0.9 together with their best fit models. Right: Spectra of the SNR 1E0102.2–7219 derived from trap corrected (red) and non-trap corrected data (black), fit with the IACHEC model.

Table 2: XRT PC (grade 0 – 12) and XMM PN (pattern 0 – 4) & MOS1/2 (pattern 0 – 12) spectral comparison for a simultaneous observation of 3C 273 taken on 2010-Dec-10. Model : PHABS \* (ZBBODY + ZBBODY + POWER) with NH fixed at the galactic value of  $1.67 \times 10^{20} \text{ cm}^{-2}$  (using xsect vern and abund wilm) and  $z = 0.158$ .

	PN	MOS1/2 <sup>†</sup>	XRT PC
$kT_{\text{bb},1}$ <sup>a</sup>	$0.087 \pm 0.002$	$0.112 \pm 0.004$	$0.121 \pm 0.038$
$N_{\text{bb},1}$ <sup>b</sup>	$3.55 \pm 0.11$	$2.55 \pm 0.15$	$2.41 \pm 0.91$
$kT_{\text{bb},2}$ <sup>a</sup>	$0.227 \pm 0.008$	$0.306 \pm 0.013$	$0.29 \pm 0.14$
$N_{\text{bb},2}$ <sup>b</sup>	$1.35 \pm 0.07$	$3.55 \pm 0.15$	$1.03 \pm 0.73$
$\Gamma$ <sup>c</sup>	$1.539 \pm 0.008$	$1.424 \pm 0.020$	$1.39 \pm 0.07$
$N_{\text{PL}}$ <sup>d</sup>	$1.77 \pm 0.02$	$1.65 \pm 0.05$	$1.80 \pm 0.22$
$F_x$ <sup>e</sup>	$1.538 \pm 0.004$	$1.629 \pm 0.008$ (M1)	$1.81 \pm 0.03$
		$1.647 \pm 0.008$ (M2)	

<sup>†</sup> MOS1/2 were jointly fit; <sup>a</sup> zbbody temperature (eV); <sup>b</sup> zbbody normalisation ( $\times 10^{-4}$ ); <sup>c</sup> powerlaw photon index; <sup>d</sup> powerlaw normalisation ( $\times 10^{-2}$ ); <sup>e</sup> 0.3 – 10 keV observed flux ( $\times 10^{-10} \text{ erg cm}^{-2} \text{ s}^{-1}$ )

The PC  $V_{ss} = 6 \text{ V}$  RMF/ARF combination was tested in the following ways:

- (i) Spectra of the soft neutron star source RX J1856.5–3754 from 2007-Sep to 2010-Aug, modelled with a 63 eV blackbody, return a flux within 8 per cent of that expected for this source (Beuermann et al., 2006, A&A, 458, 541).
- (ii) Observations of the O and Ne line rich SNR 1E0102.2–7219 from 2008-Oct to 2010-Sep, returns a normalisation within 10 per cent when fit with the IACHEC model of Plucinsky et al. (2008, SPIE, 7011).
- (iii) The spectrum of the absorbed source SNR G21.5–0.9, accumulated from 2007-Oct to 2010-Jul, can be fit with a column density of  $3.10 \pm 0.06 \times 10^{22} \text{ cm}^{-2}$ , a photon index of  $1.82 \pm 0.03$  and a 2 – 8 keV unabsorbed flux of  $5.58 \pm 0.04 \times 10^{-9} \text{ erg cm}^{-2} \text{ s}^{-1}$ , in excellent agreement with the cross-calibration work of Tsujimoto et al. (2011, A&A, 525, A25).
- (iv) An observation of the quasar 3C 273 taken simultaneously with XMM on 2010-Dec-10 shows good agreement between the XRT PC mode and MOS1/2 data (see table 2), with fluxes consistent at the 10 per cent level.

Overall, our tests show a typical photon index 2 powerlaw-like spectrum will return a photon index that decreases by  $\sim 0.1 - 0.15$  when the new PC mode RMF is used.

## Windowed Timing mode

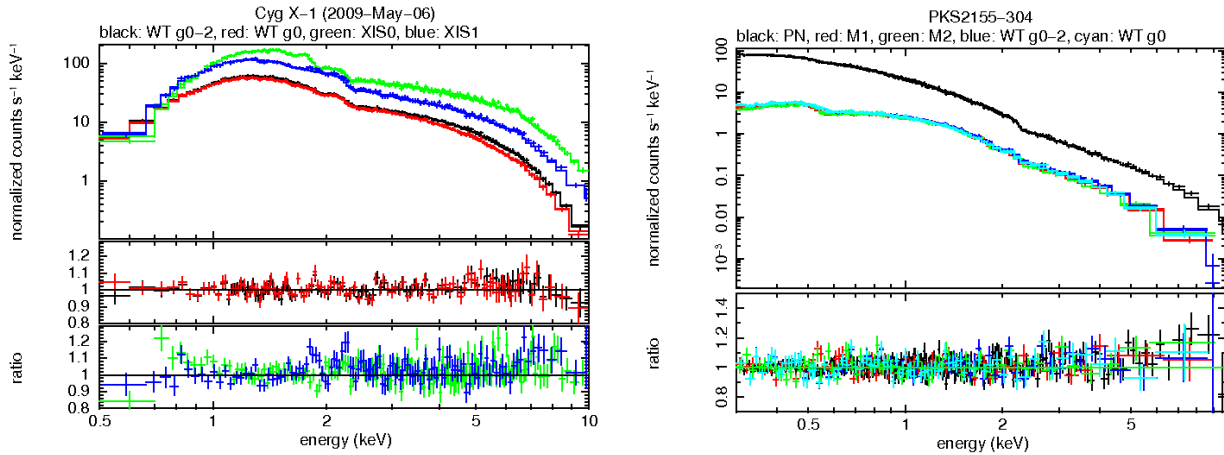


Figure 2: Left: XRT WT (grade 0 – 2 in black, grade 0 in red, fit with the new v013 RMF/ARF) and Suzaku XIS0 (green), XIS1 (blue) spectra from a simultaneous observation of Cyg X-1 on 2009-May-06. Right: XRT WT (grade 0 – 2 in blue, grade 0 in cyan), XMM PN (black), MOS1 (red) and MOS2 (green) spectra from a simultaneous observation of PKS 2155–304 on 2009-May-28.

For Windowed Timing (WT) mode, we found the previously released  $V_{ss} = 6$  V RMF, described in SWIFT-XRT-CALDB-09\_v14, and which is broadened to a level appropriate for post 2007-Sep epoch data, works well with the trap-corrected WT spectra. However, two minor changes were made to this RMF: (i) the asymmetric function used to broaden the RMF was found to shift the redistribution kernel by 15 eV to lower energies. To compensate for this, we modified the RMF by shifting the response by one Pulse Invariant (PI) channel (10 eV). (ii) Minor corrections were made around to the QE the Si edge based on high statistical quality, trap-corrected observations of the blazar Mrk 421.

Table 3: XRT WT and Suzaku XIS0/1 spectral fit results from a simultaneous observation of Cyg X-1 obtained on 2009-May-06. Model: PHABS \* (DISKBB + POWERLAW).

Instrument	XIS0/1	XRT WT	
		grade 0 – 2	grade 0
NH <sup>a</sup>	$0.857 \pm 0.054$	$0.852 \pm 0.053$	$0.799 \pm 0.050$
diskbb $kT$ <sup>b</sup>	$0.223 \pm 0.017$	$0.218 \pm 0.020$	$0.234 \pm 0.025$
diskbb norm <sup>c</sup>	$2.05^{+1.58}_{-0.92}$	$1.57^{+1.38}_{-0.76}$	$0.82^{+0.86}_{-0.43}$
photon index, $\Gamma$	$1.795 \pm 0.028$	$1.736 \pm 0.031$	$1.737 \pm 0.033$
$F_x$ <sup>d</sup>	$11.08^{+0.07}_{-0.22}$ (XIS0)	$9.46^{+0.06}_{-0.14}$	$9.35^{+0.08}_{-0.19}$
	$10.55^{+0.07}_{-0.22}$ (XIS1)		

<sup>a</sup> Column density ( $\times 10^{22} \text{ cm}^{-2}$ ); <sup>b</sup> Disc blackbody temperature (keV); <sup>c</sup> Disc blackbody normalisation ( $\times 10^9$ ); <sup>d</sup> 0.5 – 10 keV flux ( $\times 10^{-9} \text{ erg cm}^{-2} \text{ s}^{-1}$ )

The WT RMF/ARF combination was tested in the following ways :

- (i) Table 3 compares the parameters obtained when fitting the XRT and Suzaku XIS0/1 spectra from Cyg X-1, observed simultaneously on 2009-May-06, showing good agreement between the instruments (see figure 2(a)).
- (ii) Table 4 shows a comparison of the spectral fit results obtained for the blazar PKS 2155–304 from data taken simultaneously with XMM MOS1/MOS2/PN on 2009-May-28 (see figure 2(b)).

## Current limitations and future prospects

Experience has shown that the RMF/ARFs described here can be used reliably over the energy range 0.3 – 10 keV (but see the caveat below). A systematic error of about 3 per cent is needed for high statistical quality spectra for these response files.

Table 4: XRT WT and XMM MOS1/MOS2/PN spectral comparison for a simultaneous observation of PKS 2155–304 taken on 2009-May-28. Model : PHABS \* BKNPOW with NH fixed at the galactic value of  $1.48 \times 10^{20} \text{ cm}^{-2}$ .

	MOS1	MOS2	PN	XRT WT	
				grade 0 – 2	grade 0
$\Gamma_1^a$	$2.509 \pm 0.055$	$2.540 \pm 0.115$	$2.684 \pm 0.030$	$2.404 \pm 0.100$	$2.426 \pm 0.097$
$E_b^b$	$1.211 \pm 0.120$	$1.176 \pm 0.180$	$1.033 \pm 0.070$	$1.129 \pm 0.165$	$1.161 \pm 0.170$
$\Gamma_2^c$	$2.844 \pm 0.048$	$2.925 \pm 0.060$	$2.882 \pm 0.016$	$2.816 \pm 0.055$	$2.830 \pm 0.056$
$N_H^d$	$0.09 \pm 0.01$	$1.02 \pm 0.09$	$1.294 \pm 0.030$	$2.11 \pm 0.81$	$2.30 \pm 0.71$
$F_x^e$	$1.23 \pm 0.02$	$1.22 \pm 0.02$	$1.274 \pm 0.006$	$1.17 \pm 0.01$	$1.17 \pm 0.02$

<sup>a</sup> photon index below the break; <sup>b</sup> break energy; <sup>c</sup> photon index above the break; <sup>d</sup> Column density ( $\times 10^{20} \text{ cm}^{-2}$ ). Cf. Galactic value of  $1.48 \times 10^{20} \text{ cm}^{-2}$ ; <sup>e</sup> 0.3 – 10 keV observed flux ( $\times 10^{-10} \text{ erg cm}^{-2} \text{ s}^{-1}$ )

The following considerations apply when using the RMFs/ARFs described here:

- WT data suffer from a redistribution problem for spectra from heavily absorbed sources with a column density in excess of a  $\sim 10^{22} \text{ cm}^{-2}$ . The problem manifests itself as a ‘bump’ at low energies (typically below 1 keV) in the grade 0–2 spectrum from such sources, with a ‘turn-up’ at the low energy end (below  $\sim 0.4 \text{ keV}$ ). The bump is a consequence of heavy redistribution occurring in WT grade 1 and 2 events which are then cut off quickly by the onboard event threshold. Grade 0 events do not show the bump, though the turn-up is still present. If a heavily absorbed source has been observed in WT mode we recommend comparing its grade 0 and grade 0–2 spectra and if differences below  $\sim 1 \text{ keV}$  are apparent to use the grade 0 spectrum for further analysis. We will address this WT redistribution issue in a future release of the WT RMF.
- Whilst the latest version of the XRTCALCPI software performs corrections for the deepest traps (larger than 20 eV), which helps minimise the residuals around the instrumental edges, some observations still show 10 per cent residuals near the oxygen edge at 0.545 keV, and to a lesser extent the Silicon edge at 1.839 keV, especially in WT mode. Such residuals can often be improved through careful use of the *gain fit* command in XSPEC by allowing the gain offset to vary by  $\sim \pm 10 - 20 \text{ eV}$ .
- The trap offsets have been measured to be deeper in WT mode than PC mode, which means there is more scope for low energy events to be lost below the event threshold in WT mode. This is particularly evident in spectra of the soft NS source RX J1856.5–3754, which has a blackbody spectrum of temperature 63 eV, whose spectra can only be fit above  $\sim 0.35 \text{ keV}$ , and which recently recovers a constant factor of 0.76 (i.e. a reduced flux) compared with the model of Beuermann et al. (2006, A&A, 458, 541). Consequently, care is needed when using data below 0.35 keV in WT mode.
- While the current trap-correction methods provide the best spectral resolution possible for the XRT, we expect the number or shallower traps (i.e. those below our measurement capability) to slowly increase, and hence the spectral broadening to slowly evolve, though at a much slower rate than for non trap-corrected data. We will continue to monitor the spectral performance of the XRT and release RMFs with updated broadening if, or when, they become necessary.

## Useful Links

Summary of XRT RMF/ARF releases	<a href="http://www.swift.ac.uk/Gain_RMF_releases.html">http://www.swift.ac.uk/Gain_RMF_releases.html</a>
XRT analysis at GSFC	<a href="http://swift.gsfc.nasa.gov/docs/swift/analysis">http://swift.gsfc.nasa.gov/docs/swift/analysis</a>
XRT analysis threads at U. Leicester	<a href="http://www.swift.ac.uk/XRT.shtml">http://www.swift.ac.uk/XRT.shtml</a>
XRT digest pages at U. Leicester	<a href="http://www.swift.ac.uk/xrtdigest.shtml">http://www.swift.ac.uk/xrtdigest.shtml</a>
IACHEC website	<a href="http://web.mit.edu/iachec/">http://web.mit.edu/iachec/</a>